1 **Motion-correlated flow distortion and wave-induced biases**
2 **in air-sea flux measurements from ships**

3
4 **John Prytherch[1], Margaret J. Yelland[2], Ian M. Brooks[1], David J. Tupman[1,*],**

5 **Robin W. Pascal[2], Bengamin I. Moat[2], Sarah J. Norris[1].**

6

7 [1]{ School of Earth and Environment, University of Leeds, Leeds, UK}

8 [2]{National Oceanography Centre, Southampton, UK}

9 [*]{now at Centre for Applied Geosciences, University of Tuebingen, Germany}

10

11 Correspondence to: J. Prytherch (J.Prytherch@leeds.ac.uk)

12

13

14   **Abstract**

15   Direct measurements of the turbulent air-sea fluxes of momentum, heat, moisture and gases

16   are often made using sensors mounted on ships. Ship-based turbulent wind measurements are

17   corrected for platform motion using well established techniques, but biases at scales

18   associated with wave and platform motion are often still apparent in the flux measurements.

19   It has been uncertain whether this signal is due to time-varying distortion of the air flow over

20   the platform, or to wind-wave interactions impacting the turbulence. Methods for removing

21   such motion-scale biases from scalar measurements have previously been published but their

22   application to momentum flux measurements remains controversial. Here we show that the

23   measured motion-scale bias has a dependence on the horizontal ship velocity, and that a

24   correction for it reduces the dependence of the measured momentum flux on the orientation

25   of the ship to the wind. We conclude that the bias is due to experimental error, and that time-

26   varying motion-dependent flow distortion is the likely source.

27

28   **1. Introduction**

29   Obtaining direct eddy covariance estimates of turbulent air-sea fluxes from ship-mounted

30   sensors is extremely challenging. Measurements of the turbulent wind components must be

31   corrected for the effects of platform motion and changing orientation (Edson et al., 1998;

32   Schulze et al., 2005; Brooks, 2008; Miller et al., 2008). The ship also acts as an obstacle to

33   the air flow forcing it to lift and change speed; this results in both the measured mean wind

34   being biased (accelerated/decelerated) relative to the upstream flow and the effective

35   measurement height being lower than the instrument height. This can significantly bias

36   estimates of the 10 m neutral wind speed (U_{10n}) and the surface exchange coefficients

37   (Yelland et al., 1998). Computational fluid dynamics (CFD) modelling studies of the flow

38   distortion have been used to determine corrections for these mean flow distortion effects for a

39   number of different research vessels (Yelland et al., 1998, 2002; Dupuis et al., 2003; Popinet

40   et al., 2004; Moat et al., 2005; O'Sullivan et al., 2013, 2015) and also generic corrections for

41   commercial vessels that report meteorological measurements (Moat et al., 2006a,b).

42   The modelled corrections show a strong dependence on the relative wind direction

43   (Yelland et al., 2002; Dupuis et al., 2003) and a much weaker dependence on wind speed, but

44   in general have been determined only for ships with zero pitch and roll angles. Weill et al.

45   (2003) and Brut et al. (2005) reported on experiments with a 1/60 scale physical model of the

46   *RV La Thalassa* to investigate the effect of pitch and roll angles on the mean flow distortion.

2

47 They found the tilt of the mean streamline to vary by more than 1° and the mean wind speed

48 by up to 12% for pitch angles between ±10°; these effects were asymmetric about zero pitch.

49 Roll angle had only a small impact on the measured wind speed, about 1% for roll of up to

50 10°, but this was examined for bow-on flows only and a larger impact might be expected for

51 flows with a significant beam-on component. Comparison of in situ measurements from sonic

52 anemometers, the physical model tests, and CFD modelling also revealed that the foremast

53 itself, along with the instruments and electronics enclosures mounted on it, had a significant

54 impact on flow distortion at the location of the sonic anemometer.

55   The studies of flow distortion cited above addressed only the mean flow for a fixed

56 orientation of the ship with respect to the mean streamline; to the best of our knowledge no

57 studies have investigated the effect of time-varying flow distortion as ship attitude changes.

58 That the time-varying flow distortion has an impact can, however, be inferred from reported

59 biases of ship-based eddy covariance measurements. Edson et al. (1998) compared eddy

60 covariance estimates of the kinematic wind stress from two ships with those from a small

61 catamaran and from the stable research platform FLIP. They found that the ship-based

62 estimates were on average 15% higher than those from FLIP and the catamaran. They argued

63 that the difference resulted from flow distortion over the ship rather than from inadequate

64 motion correction because the catamaran experienced more severe platform motion. Pedreros

65 et al. (2003) similarly found momentum flux estimates from a ship to be 18% higher than

66 estimates from a nearby air-sea interaction spar buoy. Evidence of such biases, ascribed to

67 flow distortion, led to the exclusion of ship-based direct flux measurements from the most

68 recent update of the COARE bulk air-sea flux algorithm (v3.5; Edson et al., 2013).

69   Features in cospectra that manifest as significant deviations from the expected

70 spectral form (e.g. Kaimal et al., 1972) at frequencies associated with waves and platform

71 motion have been reported in observations of momentum fluxes measured from FLIP (Miller

72 et al., 2008) and from fixed platforms (Deleonibus, 1971) and towers (Drennan et al., 1999).

73 A decrease in the magnitude of the feature with height led Miller et al. (2008) to ascribe its

74 source to interactions between the waves and atmospheric turbulence. The authors also note

75 that the anemometers used were not co-mounted with inertial motion units and their tilt from

76 horizontal was determined using the planar fit method; errors in the determined tilt or in

77 estimation of anemometer and inertial motion unit alignment could also contribute to the

78 observed features via incomplete correction for platform motion (Brooks, 2008; Landwehr et

79 al., 2015). Edson et al. (2013) analysed wind profile measurements from three field

80 campaigns and found little evidence of wave influence on winds at heights above 4 m in sea

81   conditions with $c_p/U_{10n} < 2.5$, where c_p is the wave phase speed. In general, reported motion-

82   scale signals in the turbulence have been observed in measurements made either at heights

83   below 10 m (Deleonibus, 1971; Miller et al., 2008) or in conditions of fast, high swell where

84     $c_p/U_{10n} \approx 2$ and $Hs_{swell} >> Hs_{wind}$, and Hs_{swell} and Hs_{wind} are the significant wave heights of the

85   swell and wind-wave components of the wave field respectively (Drennan et al., 1999).

86   Recent results from Large Eddy Simulations over moving wave fields also suggest that, in

87   developing sea conditions waves are not expected to significantly influence turbulent winds

88   at heights of more than about 10 m (Sullivan et al., 2014). In summary, the wave field is only

89   expected to influence the turbulent winds near the surface or in conditions where swell

90   dominates the wave field.

91   High frequency gas concentration measurements for studies of air-sea exchange have

92   been shown to suffer significant motion-correlated biases resulting from the hydrostatic

93   pressure change with vertical displacement (Miller et al., 2010), and potentially from

94   mechanical sensitivities of the sensors themselves (McGillis et al., 2001; Yelland et al., 2009;

95   Miller et al., 2010). These biases cause distortions of the cospectra between the vertical wind

96   component and gas concentration (Edson et al., 2011) apparent in the cospectra at frequencies

97   associated with the platform motion, and several recent studies have applied motion

98   decorrelation algorithms to remove this signal (Miller et al., 2010; Edson et al., 2011;

99   Blomquist et al., 2014).

100   Such an approach can also correct the apparent motion-scale bias in the momentum

101   flux, but is controversial since, as discussed above, there are circumstances in which a real

102   wave-correlated signal may be expected in the turbulence measurements. Here we present

103   measurements which demonstrate a significant motion-scale feature in momentum flux

104   measurements from a research ship. We show the impact of applying a simple regression

105   procedure to remove the bias, and provide evidence that suggests the source of the bias is

106   time-varying flow distortion correlated with ship motion and attitude.

107

108   **2. Data**

109   The measurements were made on the *RRS James Clark Ross* as part of the Waves, Aerosol

110   and Gas Exchange Study (WAGES), a programme of near-continuous measurements using

111   the autonomous AutoFlux system (Yelland et al., 2009). Turbulent wind components were

112   measured by a Gill R3 sonic anemometer installed above the forward, starboard corner of the

113   ship's foremast platform (Fig. 1). The measurement volume was approximately 16.5 m above

114   sea level. Platform motion was measured with a Systron Donner MotionPak Mk II, mounted

115   rigidly at the base of the anemometer and sampled synchronously with it. Wave field

116   measurements were made using a WAVEX X-band radar installed above the bridge top. The

117   WAVEX system obtains directional wave spectra and mean wave parameters every five

118   minutes.

119   The fast-response instrumentation operated at 20 Hz, and flux estimates were

120   calculated over 30-minute periods. The raw wind and motion measurements were first

121   despiked and the wind components corrected for platform motion using the complementary

122   filtering approach of Edson et al. (1998). The motion correction algorithm set out in Edson et

123   al. (1998) and as usually applied corrects the measured horizontal winds for low frequency

124   horizontal motions (ship's underway velocity) in the earth frame. This neglects the aliasing of

125   the ship's horizontal speed into the vertical imposed by the non-horizontal mean streamline at

126   the point of measurement due to flow distortion over the ship. The true vertical wind speed,

127   w_{true} is determined from the measured, motion-corrected vertical wind, w_{rel}, and the

128   horizontal true and relative winds (U_{true} and U_{rel}) as

129

130    $$w_{true} = w_{rel} - \left(\overline{w_{rel}} \times \left[1 - \overline{U_{true}} \Big/ \overline{U_{rel}} \right] \right) \qquad (1)$$

131

132   where overbars indicate a time average (Tupman, 2013). The derivation of Eq. (1) and the

133   impact of applying this correction are described in Appendix A. This correction addresses the

134   same source of measurement error as that recently described by Landwehr et al. (2015) who

135   address it by applying corrections for the ship's low-frequency horizontal velocity after

136   rotating the ship-relative winds (corrected for high frequency motions) into the reference

137   frame of the mean streamline for each flux averaging period.

138   After motion correction, each 30-minute record is rotated into a reference frame

139   aligned with the mean streamline, wind components were linearly detrended, and eddy

140   covariance momentum fluxes calculated. CFD modelling of the air flow over the James Clark

141   Ross was initially undertaken by Yelland et al. (2002), but only for flow on to the bow; we

142   have extended the CFD study for a much wider range of relative wind directions and the

143   results were used to determine direction-dependent corrections to the mean (30-minute

144   averaged) relative wind speed and measurement height. The new CFD study is documented

145   in Moat and Yelland (2015) and the primary results reproduced here in Appendix B. The

146   modelled wind speed bias at the sensor location varied between -0.9% and 8.4% for wind

147   directions between 20° to port of the bow and 120° to starboard, and the height by which the

148 flow was raised varied between 1.3 m and 3.2 m. Wind directions beyond 20° to port of the

149 bow were affected by small-scale obstructions on the foremast platform that are not included

150 in the CFD model; these wind directions are thus excluded from the following analysis. After

151 applying the corrections, the measured winds were corrected to 10 m height and neutral

152 stability using the Businger-Dyer relationships (Businger, 1988) and the 10 m neutral drag

153 coefficient, CD_{10n}, was calculated from U_{10n} and the momentum flux estimates.

154   The measurements used here were obtained between 09 January and 16 August, 2013

155 in locations throughout the North and South Atlantic, the Southern Ocean and the Arctic

156 Ocean, at latitudes ranging from 62°S to 75°N. After excluding measurement periods when

157 the ship was within sea ice, there were 2920 individual flux estimates available for analysis.

158 Flux estimates were then rejected from the analysis where there was excessive ship

159 manoeuvring, where flux quality control criteria were failed (Foken and Wichura, 1996;

160 Vickers and Mahrt, 1997), and when the air temperature was less than 2°C when ice build up

161 may affect the sensors. Of the remaining 1054 flux estimates, 80 were removed as outliers

162 ($CD_{10n} > 5 \times 10^{-3}$). Unless otherwise indicated, mean relative wind direction limits of 20° to

163 port, and 50° to starboard of the bow were applied, a condition met by 499 flux estimates. Of

164 the removed outliers, 38 lay within acceptable relative wind direction limits; of these, 6 were

165 at winds speeds of 6 m.s^{-1} or greater.

166

3. Removal of the ship motion-scale signal

168 Momentum flux cospectra and ogives for U_{10n} between 10 and 14 m s^{-1}, normalised (by f/u_*^2

169 and $1/u_*^2$ respectively, where f is frequency and u_* is the friction velocity) and averaged, are

170 shown in Fig. 2. The cospectra and ogives differ from the typical forms obtained from

171 experiments over land (e.g. Kaimal et al., 1972) at frequencies between approximately 0.06

172 and 0.25 Hz (0.09 and 0.37 in the non-dimensionalised frequency shown in Fig. 2), where a

173 significant anomalous signal is present. These are frequencies associated with surface waves

174 and with the platform motion that results, hence we term the cospectral signal at these

175 frequencies the motion-scale signal.

176   At wind speeds above 7 m s^{-1}, the CD_{10n} measurements are biased high compared

177 with previous results (Fig. 3). The bias relative to the eddy covariance parameterisation of

178 Smith (1980) increases with wind speed from approximately 20% at 8 m s^{-1} to 60% at 20 m s^{-}

179 ^{1}. Note that the Smith (1980) parameterisation was derived from eddy covariance

180 measurements made from a slim floating tower moored so as to minimise platform motion

181 and inducing minimal flow distortion. The bias is smaller when compared to the COARE 3.0

182 (Fairall et al., 2003) or COARE 3.5 (Edson et al., 2013) bulk algorithms.

183   The motion-scale signal can be removed from the vertical wind component, and a

184 corrected vertical wind, w_{MSC}, obtained via a simple regression method:

185

186 $$w'_{MSC} = w'_{true} - \alpha_1 acc'_z - \alpha_2 vel'_z \qquad\qquad (2)$$

187

188 where acc_z and vel_z are the platform's vertical acceleration and velocity, measured at the base

189 of the sonic anemometer, and primes denote fluctuations determined from Reynolds

190 decomposition. The coefficients α_1 and α_2 are determined here by regression for each 30-

191 minute flux measurement period. This algorithm, which we term the motion-scale correction

192 (MSC), is based on the regression corrections of Yelland et al., (2009) and Miller et al.,

193 (2010). It is also similar to the motion decorrelation algorithm given in a spectral formulation

194 by Edson et al. (2011), originally utilised to remove motion biases from CO_2 flux cospectra,

195 and here termed the MSC_f. The MSC_f algorithm coefficients are defined as the ratio of

196 covariances of vertical wind and platform motion to variances of platform motion. The MSC

197 and MSC_f methods give almost identical results (Fig. 2).

198   Applying the MSC algorithm removes the motion-scale signal (Fig. 2) and results in a

199 20% to 30% decrease in CD_{10n} for wind speeds above 7 m s^{-1} and absolute values similar to

200 those of COARE 3.0 or 3.5 (Fig. 3). The signal removed is similar in size and of the same

201 sign as the biases in ship-based momentum flux measurements reported by Edson et al.

202 (1998) and Dupuis et al. (2003).

203   Applying the MSC to the along-wind component as well as the vertical component

204 makes an insignificant (<<1%) additional difference to the measured flux (shown as MSC_{uv}

205 in Figs. 2 and 3). Interpolating the measured cospectra across the motion-scale frequencies

206 gives similar results to the MSC algorithm under most conditions (shown as "interpolated" in

207 Figs. 2 and 3: Prytherch, 2011; Tupman, 2013). However, interpolation requires selection of

208 appropriate frequencies to interpolate between, in this case 0.04 and 0.4 Hz (0.06 and 0.59 in

209 the non-dimensionalised frequency shown in Fig. 2), and is not dependent on a physical

210 variable related to the presumed source of the error (platform motion-dependent flow

211 distortion). For these reasons, correction using the MSC algorithm is preferable.

212

213 **4. Discussion**

214   Following application of the MSC the cospectral shape matches the Kaimal form expected.

215   This suggests that the motion-scale bias is being effectively removed.

216   The MSC also results in drag coefficients that lie within the range of previous

217   parameterisations. At the highest wind speeds (over 15 m s^{-1}) the parameterisations begin to

218   diverge significantly and the WAGES CD_{10n} are larger than those given by Smith (1980) and

219   lie between those of COARE 3.0 and 3.5. It should be noted that COARE 3.0 and 3.5 are

220   both defined using wind speeds in the frame of reference of the surface currents (see

221   Appendix in Edson et al., 2013), rather than in the earth frame of reference as used by Smith

222   (1980). Surface current measurements were not available for the WAGES data. For surface

223   currents aligned with the prevailing wind direction, adopting a surface current frame of

224   reference would lead to a small apparent increase in the drag coefficients presented here.

225   While several previous studies have ascribed a high bias in drag coefficient estimates

226   from ships to flow distortion (Edson et al. 1998, 2013; Pedreros et al. 2003), they have not

227   examined the effect in detail. Inaccurate tilt estimation, a related source of error, may also

228   contribute to this bias, particularly at low wind speeds (Landwehr et al., 2015). Few other

229   studies have discussed such biases at all, and it seems likely that the severity of any motion-

230   correlated bias is highly dependent on individual platforms and instrument installations in the

231   same manner as the mean flow distortion. The bias is potentially worse here than in many

232   other studies; the sonic anemometer is mounted lower on the foremast than would be ideal

233   because the long-term measurement programme made it necessary to be able to service the

234   instruments easily and without access to a crane. There are also a greater number of small-

235   scale obstructions such as searchlights near to the measurement point than would be the case

236   on lattice style masts often deployed on dedicated flux measurement campaigns. Because the

237   measurements are continuous and autonomous, a large fraction of our data is also obtained

238   with the ship underway. In contrast, dedicated eddy covariance studies of air-sea exchange

239   would usually focus almost exclusively on measurements made on station when ship motion

240   is substantially less than when underway. Finally it is possible that such biases are present in

241   some fraction of the measurements of many studies, but are excluded from final analysis by

242   quality control procedures without a close examination of the bias being made. Many studies

243   with modest data volumes have quality controlled the individual flux estimates via a visual

244   inspection of the ogive curves, rejecting those that do not closely match the expected form

245   (e.g. Fairall et al. 1997; Norris et al. 2012).

246   As discussed in Sect. 1 above, there is evidence from previous studies that the

247   influence of the wave field on the turbulent winds should be small at heights above some

248 limit which is assumed to be related to the wave properties: values between 4 and 10 m have

249 been cited (Miller et al. 2008, Sullivan et al. 2014). The Sullivan et al. (2014) results

250 correspond to a height of order 1.5 times the significant wave height. Real wave effects are

251 thus expected to be negligible for typical measurement heights of ship-based sensors (15-20

252 m) under most conditions. Below we provide more direct evidence that the wave-scale signal

253 seen in the WAGES data is due, in large part at least, to the effects of flow distortion over a

254 moving platform.

255

256 **4.1 Motion dependence of the streamline**

257 The angle to the horizontal of the airflow measured at the sonic anemometer site was found to

258 be dependent on the vertical motion of the ship (Fig. 4). Perturbations in the tilt of the

259 streamline are approximately in phase with acc_z, out of phase with the vertical displacement

260 and pitch, and lead vel_z by about 90°. There are multiple processes that may affect the

261 streamline orientation as the ship moves over the waves:

- 262 • Vertical displacement of the ship changes the vertical extent of the obstacle that the
- 263   ship presents to the flow and the relative height of the measurement volume with
- 264   respect to that of the bow above the water line.
- 265 • The ship's pitch similarly changes both the effective size of the obstacle presented to
- 266   the flow and the relative location of the sonic anemometer within the distorted flow
- 267   above the bow.
- 268 • Vertical motion of the ship will force the overlying air to move.

269

270 In the example here for 15 m s^{-1}, bow-on winds, the airflow tilt varies by about ± 3° around a

271 mean of approximately 10°. The various parameters shown in Fig. 4a are all inter-dependent,

272 but streamline tilt showed slightly more consistent trends with the velocity and acceleration

273 parameters than with displacement or pitch suggesting that "pumping" of the air above the

274 moving deck may be the dominant effect.

275

276 **4.2 Characteristic frequencies of spectral features**

277 For a platform moving through a wave field aligned with the direction of travel, it would be

278 expected that the frequency of ship motion forced by the waves would differ from that for a

279 ship on station with no mean horizontal velocity. The change could be of either sign

280 depending on the ratio of wavelength to the length of the ship, with an increase in frequency

281   for wavelengths much longer than the ship. The measured frequency of atmospheric turbulent

282   structures would also be shifted to higher frequencies relative to those measured when on

283   station. The nature of the frequency shift should differ for turbulent air motions, which advect

284   with the wind and have a ship-relative velocity equal to the sum of wind and ship speeds, and

285   wave-correlated features in the turbulence field which are phase-locked to the surface waves

286   (Sullivan et al. 2000; 2008; 2014), and will have a ship-relative velocity of the sum of wave-

287   phase and ship speeds. A signal due to real wind-wave interaction should thus appear at a

288   different frequency to that from a ship motion-induced measurement bias.

289   Figure 5 shows a comparison of the power spectral density of platform vertical

290   velocity (S_{velz}, Fig. 5b) and frequency weighted cospectral densities for the streamwise

291   momentum flux (normalised by u_*) both for periods during which the ship was on station

292   ($V_{ship} < 1$ m s^{-1}, where V_{ship} is the speed of the ship) and when underway ($V_{ship} > 5$ m s^{-1}). The

293   cospectra are shown after applying the standard motion correction to the measured turbulent

294   velocity components, but without applying the MSC correction. Also shown are the spectral

295   densities of the surface wave field (Fig. 5a). The wave radar provides wave spectra in the

296   earth frame, corrected for ship speed; in order to compare these directly with the measured

297   turbulence and ship-motion spectra when underway we need to transform them into a

298   reference frame moving with the ship. This is achieved by plotting against a modified

299   frequency, $f_m = f_0(c_p + V_{ship})/c_p$, where f_m is the frequency that would be measured in the ship

300   reference frame and f_0 is the true frequency in the earth frame. The periods chosen all have

301   bow-on winds, wind speeds of between 10 and 12 m s^{-1} and similar sea states: the (true) mean

302   peaks of the mean WAVEX-derived non-directional wave spectra (S_{zwave}) are 0.120 and 0.110

303   Hz, and mean significant wave heights are 4.73 m and 3.51 m for the stationary and

304   underway periods respectively.

305   For the on station measurements, the peak in the momentum flux cospectra (no MSC,

306   Fig. 5c) is at 0.113 Hz, which matches that of the peak in ship vertical velocity (Fig. 5b) and

307   is at slightly lower frequency than the peak in the ship-frame surface wave spectra (0.120 Hz,

308   Fig. 5a). For the underway cases the peak in the ship-frame wave spectra is shifted to higher

309   frequency (0.163 Hz) compared to the true spectra. The peak in the ship motion spectrum

310   (0.148 Hz) is again lower than that of the wave spectrum and by a larger margin than for the

311   on station case. The peak in the momentum flux cospectrum at 0.153 Hz is much closer to

312   that of the ship motion than that of the wave spectrum.

313   The correspondence of the peak in momentum flux cospectra with that of the ship

314   motion rather than that of the wave field suggest that the residual signal after motion

315   correction is an artefact of motion-correlated flow distortion rather than a result of a real

316   wave-correlated signal in the turbulence.

317

318   **4.3   Directional dependence of drag coefficient bias**

319   Mean flow distortion is strongly dependent on relative wind direction (Yelland et al., 1998),

320   even for a motionless ship with zero pitch and roll angles. The dependence of the calculated

321   drag coefficients on relative wind direction before and after applying the MSC algorithm is

322   shown in Fig. 6. First, a linear fit was made between the drag coefficient and wind speed data

323   obtained for wind directions between -20 and +50 degrees of the bow. Then the drag

324   coefficient anomalies (individual minus fit) were calculated and averaged into 10° relative

325   wind direction bins, and the results were plotted against relative wind direction. It can be seen

326   that prior to applying the MSC algorithm the drag coefficient anomalies have a significant

327   dependence on relative wind direction, and that application of the algorithm significantly

328   reduces this dependence. For completeness the results are also shown without first applying

329   the direction-dependent CFD-derived correction to the mean, 30-minute averaged, wind

330   speed; this also reduces the dependence of the drag coefficient on relative wind direction.

331   Application of the MSC and the mean CFD correction does not completely remove all

332   dependence of the drag coefficient on relative wind direction. This suggests that one or both

333   corrections may need refinement. In the case of the MSC algorithm, the effect of the roll of

334   the ship is likely to become significant when the wind direction is beam-on rather than bow-

335   on. In the case of the CFD correction to the mean wind speed, the model of the ship geometry

336   may have to be refined to take into account local flow distortion caused by small objects

337   mounted on the foremast, close to the anemometer. These are areas for future investigation.

338

339   **5. Conclusions**

340   Methods for removal of motion-correlated signals from fast-response gas measurements

341   made onboard moving platforms have become more commonly applied in recent years;

342   however, these techniques remain controversial when applied to fast-response winds for the

343   purpose of momentum flux calculation. The results here demonstrate these methods and their

344   impact on ship-based momentum flux measurements where a significant motion-correlated

345   bias is present in the motion-corrected cospectra. The motion-correlated signals are shown to

346   be dependent on platform velocity relative to the wave field. In addition, the dependence of

347   the flux on wind direction relative to the ship is reduced after applying the correction

348   methods. These results suggest that the motion-correlated signal is due to the effects of time-
349   varying flow distortion. Further investigation is required to resolve the details of the physical
350   processes involved.

351   The recent revision of the COARE bulk flux algorithm (COARE 3.5, Edson et al.
352   2013) is determined only from data from platforms other than ships (buoys, towers, FLIP).
353   These data all require motion correction, and Bigorre et al. (2013) report biases of a few
354   percent in mean wind speed due to flow distortion around one of the buoys used to collect
355   data at high wind speed, but these platforms generally do not suffer such significant flow
356   distortion problems as ships.

357   For many applications ship-based measurements are the only option; for example,
358   direct eddy covariance measurements of gas transfer require instrumentation that can only
359   realistically be operated on a ship. A means of effectively dealing with biases induced by
360   flow distortion around a moving platform is thus essential. The methods demonstrated above
361   provide a successful correction; after its application the shape of the cospectra matches the
362   Kaimal form expected and our drag coefficient results lie within the range of recent leading
363   parameterisations.

364

365   **Appendix A. Underway vertical wind speed**
366   The motion correction algorithm of Edson et al. (1998) calculates a total platform velocity in
367   the earth frame as the sum of highpass filtered wave-induced motions, obtained from the
368   integration of accelerometers, and lowpass filtered velocities (the platform's underway
369   motion). The latter are applied only in the horizontal since the mean vertical velocity is zero
370   by definition. The corrected winds in the earth frame are obtained as the vector sum of
371   measured and platform velocities. This neglects the impact of flow distortion on the measured
372   winds (Fig. A1). At the point of measurement on the foremast of a ship, the mean flow is
373   forced to lift resulting in a streamline tilted upwards from the horizontal. The measured
374   along-streamline wind depends upon ship velocity as well as earth-relative wind. Since the
375   streamline is tilted, a fraction of the ship velocity affects the measured vertical as well as the
376   horizontal winds in the earth frame and must be corrected.

377   When conditions are stationary (an implicit assumption for direct flux measurement)
378   the measured, motion-corrected vertical wind, w_{rel}, can be corrected for the horizontal
379   platform mean velocity to obtain the true vertical wind speed w_{true}. The ratio of the mean true
380   to mean relative vertical winds is equal to the ratio of the mean true to mean relative
381   horizontal winds, i.e.

$$\frac{\overline{U_{true}}}{\overline{U_{rel}}} = \frac{\overline{w_{true}}}{\overline{w_{rel}}} \qquad \text{(A1)}$$

(Fig. A1). Then, as

$$w_{true} = w_{rel} - \left(\overline{w_{rel}} - \overline{w_{true}} \right) \qquad \text{(A2)}$$

w_{true} can be determined via Eq. (1)

$$w_{true} = w_{rel} - \left(\overline{w_{rel}} \times \left[1 - \overline{U_{true}} / \overline{U_{rel}} \right] \right).$$

Note that this affects the mean vertical wind only, not the high frequency perturbations; however failure to account for the impact of flow distortion on the vertical wind measurements would result in the streamline orientation being incorrectly calculated, and both u' and w' values being biased after rotation into the streamline-oriented reference frame in which the fluxes are calculated. We also note that at low wind speeds ($\sim < 5$ m s^{-1}), the determination of the reference frame for a particular measurement interval may be biased by offsets in the vertical wind speed, leading to errors in the tilt calculation (Wilczak et al., 2001; Landwehr et al., 2015).

The effectiveness of this correction is demonstrated through comparison of drag coefficients from periods when the ship was stationary ($V_{ship} < 1$ m s^{-1}) and underway ($V_{ship} > 5$ m s^{-1}). Prior to correction, measurements from the underway ship are biased high relative to the stationary measurements (Fig. A2). Following correction, the stationary and underway measurements are in very good agreement for all but the very lowest wind speeds. Furthermore, for stationary periods (where the effect is small), the corrected and uncorrected results are also in good agreement.

Appendix B. CFD corrections for flow distortion

The relative wind direction dependent CFD corrections for the mean flow distortion over the ship are given in Table B1. These are strictly valid only for the location of our sonic anemometer (1.24 m to starboard, 16.5 m above the waterline, and 5.0 m aft of the bow), but

should be broadly representative for nearby locations, and indicative of the directionally
dependent flow distortion that might be expected on any similar installation on other ships.

References

Bigorre, S. P., Weller, R. A., Edson, J. B. and Ware, J. D.: A Surface Mooring for Air–Sea
    Interaction Research in the Gulf Stream. Part II: Analysis of the Observations and Their
    Accuracies. J. Atmos. Oceanic Technol., 30, 450–469.
    doi: http://dx.doi.org/10.1175/JTECH-D-12-00078.1. 2013

Blomquist, B. W., Huebert, B. J., Fairall, C. W., Bariteau, L., Edson, J. B., Hare, J. E., and
    McGillis, W. R.: Advances in air-sea CO_2 flux measurement by eddy correlation,
    Bound.-Lay. Meteorol. 1-32, doi:10.1007/s10546-014-9926-2, 2014.

Brooks, I. M.: Spatially Distributed Measurements of Platform Motion for the Correction of
    Ship-Based Turbulent Fluxes. J. Atmos. Ocean. Tech., 25, 2007-2017,
    doi:10.1175/2008JTECHA1086.1, 2008.

Brut, A., Butet, A., Durand, P., Caniaux, G., and Planton, S.: Air–sea exchanges in the
    equatorial area from the EQUALANT99 dataset: Bulk parameterizations of turbulent
    fluxes corrected for airflow distortion, Q. J. Roy. Meteor. Soc., 131, 2497-2538,
    doi:10.1256/qj.03.185, 2005.

Businger, J. A.: A note on the Businger–Dyer profiles. Bound.-Lay. Meteorol., 42, 145–151,
    doi:10.1007/978-94-009-2935-7_11, 1988.

Deleonibus, P.: Momentum flux and wave spectra observations from an ocean tower. J.
    Geophys. Res., 76, 6506-6527, doi:10.1029/JC076i027p06506, 1971.

Drennan, W., Kahma, K., and Donelan, M.: On momentum flux and velocity spectra over
    waves. Bound.-Lay. Meteorol., 92, 489-515, doi:10.1023/A:1002054820455, 1999.

Dupuis, H., Geurin, D., Hauser, D., Weill, A., Nacass, P., Drennan, W.M., Cloche, S. and
    Graber, H.C.: Impact of flow distortion corrections on turbulent fluxes estimated by the
    inertial dissipation method during the FETCH experiment on R/V L'Atalante, J.
    Geophys. Res., 108, 8064, doi:10.1029/2001JC001075, 2003.

447   Edson, J. B., Hinton, A. A., Prada, K. E., Hare, J. E., and Fairall, C. W.: Direct covariance

448   flux estimates from mobile platforms at sea, J. Atmos. Ocean. Tech., 15, 547-562,

449   doi:10.1175/1520-0426(1998)015<0547:DCFEFM>2.0.CO;2, 1998.

450   Edson, J. B., Fairall, C. W., Bariteau, L., Zappa, C. J., Cifuentes-Lorenzen, A., McGillis, W.

451   R., Pezoa, S., Hare, J. E., and Helmig, D.: Direct covariance measurement of CO_2 gas

452   transfer velocity during the 2008 Southern Ocean Gas Exchange Experiment: Wind

453   speed dependency, J. Geophys. Res., 116, C00F10, doi:10.1029/2011JC007022, 2011.

454   Edson, J. B., Venkata Jampana, V., Weller, R. A., Bigorre, S. P., Plueddemann, A. J., Fairall,

455   C. W., Miller, S. D., Mahrt, L., Vickers, D., and Hersbach, H.: On the exchange of

456   momentum over the open ocean. J. Phys. Oceanogr., 43, 1589–1610, doi:10.1175/JPO-

457   D-12-0173.1, 2013.

458   Fairall, C. W., White, A. B., Edson, J. B., and Hare, J. E.: Integrated shipboard measurements

459   of the marine boundary layer, J. Atmos. Ocean. Tech., 14, 338–359, doi:10.1175/1520-

460   0426(1997)014<0338:ISMOTM>2.0.CO;2, 1997.

461   Fairall, C. W., Bradley, E. F. , Hare, J. E. , Grachev, A. A., and Edson J. B.: Bulk

462   parameterization of air-sea fluxes: Updates and verification for the COARE algorithm, J.

463   Clim., 16, 571–591, doi:10.1175/1520- 0442, 2003

464   Foken, T., and Wichura, B.: Tools for quality assessment of surface-based flux measurements

465   1. Agr. Forest Meteorol., 78, 83-105, doi:10.1016/0168-1923(95)02248-1, 1996.

466   Kaimal, J. C., Izumi, Y. J., Wyngaard, C., and Cote, R.: Spectral characteristics of surface-

467   layer turbulence, Q. J. Roy. Meteor. Soc., 98 (417), 563-589,

468   doi:10.1002/qj.49709841707, 1972.

469   Landwehr, S., O'Sullivan, N., and Ward, B.: Direct Flux Measurements from Mobile

470   Platforms at Sea: Motion and Air-Flow Distortion Corrections Revisited, J. Atmos.

471   Ocean. Tech., (in press), doi:10.1175/JTECH-D-14-00137.1, 2015.

472   McGillis, W. R., Edson, J. B., Hare, J. E., and Fairall, C. W.: Direct covariance air-sea CO_2

473   fluxes. J. Geophys. Res.-Oceans, 106, 16729-16745, doi:10.1029/2000JC000506, 2001.

474   Miller, S. D., Hristov, T. S., Edson, J. B., and Friehe, C. A.: Platform motion effects on

475   measurements of turbulence and air-sea exchange over the open ocean, J. Atmos. Ocean.

476   Tech., 25, 1683-1694, doi:10.1175/2008JTECHO547.1, 2008.

477   Miller, S. D., Marandino, C., and Saltzman, E. S.: Ship-based measurement of air- sea CO_2

478   exchange by eddy covariance. J. Geophys. Res.-Atmos., 115, D02304,

479   doi:10.1029/2009JD012193, 2010.

480   Moat, B. I., Yelland, M. J., Pascal, R. W., and Molland, A. F.: An overview of the airflow

distortion at anemometer sites on ships, Int. J. Climatol., 25(7), 997-1006, doi:10.1002/joc.1177, 2005.

Moat, B. I., Yelland, M. J., Pascal, R. W., and Molland, A.F.: Quantifying the airflow distortion over merchant ships. Part I: validation of a CFD model, J. Atmos. Ocean. Tech., 23(3), 341-350, doi:10.1175/JTECH1858.1, 2006a.

Moat, B. I., Yelland, M. J., and Molland, A. F.: Quantifying the airflow distortion over merchant ships. Part II: application of the model results, J. Atmos. Ocean. Tech., 23(3), 351-360, doi:10.1175/JTECH1859.1, 2006b.

Moat, B. I. and Yelland, M. J.: Airflow distortion at instrument sites on the RRS James Clark Ross during the WAGES project. National Oceanography Centre, Southampton, U.K. Internal Document No. 12. Available from http://eprints.soton.ac.uk/373216/, 2015.

Norris, S. J., Brooks, I. M., Hill, M. K., Brooks, B. J., Smith, M. H., and Sproson, D. A. J.: Eddy Covariance Measurements of the Sea Spray Aerosol Flux over the Open Ocean. J. Geophys. Res., 117, D07210, 15pp, doi:10.1029/2011JD016549, 2012.

O'Sullivan, N., Landwehr, S., and Ward, B.: Mapping flow distortion on oceanographic platforms using computational fluid dynamics. Ocean Science, 9(5), 855–866, doi:10.5194/os-9-855-2013, 2013.

O'Sullivan, N., Landwehr, S., and Ward, B.: Air-flow distortion and wave interactions: An experimental and numerical comparison. Methods Oceanogr., 12, 1–17, doi:10.1016/j.mio.2015.03.001, 2015.

Pedreros, R., Dardier, G., Dupuis, H., Graber, H. C., Drennan, W. M., Weill, A., Geurin, C., and Nacass, P.: Momentum and heat fluxes via the eddy correlation method on the R/V L'Atalante and an ASIS buoy, J. Geophys. Res., 108, C11, doi:10.1029/2002JC001449, 2003.

Popinet, S., Smith, M., and Stevens, C.: Experimental and numerical study of turbulence characteristics of airflow around a research vessel, J. Atmos. Ocean. Tech., 21, 1575-1589, doi:10.1175/1520-0426(2004)021<1575:EANSOT>2.0.CO;2, 2004.

Prytherch, J.: Measurement and parameterisation of the air-sea CO_2 flux in high winds. PhD thesis, University of Southampton, 2011.

Schulze, E. W., Sanderson, B. G., and Bradley, E. F.: Motion correction for shipborne turbulence sensors. J. Atmos. Ocean. Tech., 22, 44-69, doi:10.1175/JTECH-1685.1, 2005.

Smith, S.: Wind stress and heat flux over the ocean in gale force winds. J. Phys. Oceanogr., 10, 709–726, doi:10.1175/1520-0485(1980)010<0709:WSAHFO>2.0.CO;2, 1980.

515 Sullivan, P. P., McWilliams, J. C., and Moeng, C.-H.: Simulation of turbulent flow over
516   idealized water waves, J. Fluid. Mech., 404, 47-85, doi:10.1017/S0022112099006965,
517   2000.

518 Sullivan, P. P., Edson, J. B., Hristov, T., and McWilliams, J. C.: Large-eddy simulations and
519   observations of atmospheric marine boundary layers above non-equilibrium surface
520   waves, J. Atmos. Sci., 65, 1225-1245, doi:10.1175/2007JAS2427.1, 2008.

521 Sullivan, P. P., McWilliams, J. C., and Patton, E. G.: Large-Eddy Simulation of Marine
522   Atmospheric Boundary Layers above a Spectrum of Moving Waves. J. Atmos. Sci., 71,
523   4001–4027. doi:10.1175/JAS-D-14-0095.1, 2014.

524 Tupman, D. J.: Air-sea flux measurements over the Southern Ocean. PhD thesis, University
525   of Leeds, 2013.

526 Vickers, D., and Mahrt, L.: Quality control and flux sampling problems for tower and aircraft
527   data. J. Atmos. Ocean. Tech., 14, 512-526, doi:10.1175/1520-
528   0426(1997)014<0512:QCAFSP>2.0.CO;2, 1997.

529 Weill, A., Eymard, L., Caniaux, G., Hauser, D., Planton, S., Dupuis, H., Brut, A., Guerin, C.,
530   Nacass, P., Butet, A., Cloché, S., Perderos, R., Durand, P., Bourras, D., Giordani, H.,
531   Lachaud, G., and Bouhours. G.: Toward a Better Determination of Turbulent Air–Sea
532   Fluxes from Several Experiments, J. Climate, 16, 600-618, doi:10.1175/1520-
533   0442(2003)016<0600:TABDOT>2.0.CO;2, 2003.

534 Wilczak, J., Oncley, S. and Stage, S.: Sonic anemometer tilt correction algorithms, Bound.-
535   Lay. Meteorol., 99(1), 127–150, doi:10.1023/A:1018966204465, 2001.

536 Yelland, M. J., Moat, B. I., Taylor, P. K., Pascal, R.W., Hutchings, J. and Cornell, V. C.:
537   Wind stress measurements from the open ocean corrected for airflow distortion by the
538   ship, J. Atmos. Ocean. Tech., 28, 1511-1526, doi:10.1175/1520-
539   0485(1998)028<1511:WSMFTO>2.0.CO;2, 1998.

540 Yelland, M. J., Moat, B. I., Pascal, R. W., and Berry, D. I.: CFD model estimates of the
541   airflow distortion over research ships and the impact on momentum flux measurements,
542   J. Atmos. Ocean. Tech., 19, 1477-1499, doi:10.1175/1520-
543   0426(2002)019<1477:CMEOTA>2.0.CO;2, 2002.

544 Yelland, M., Pascal, R., Taylor, P. and Moat, B.: AutoFlux: an autonomous system for the
545   direct measurement of the air-sea fluxes of CO_2, heat and momentum. J. Operation.
546   Oceanogr., 15-23, doi:10.1080/1755876X.2009.11020105, 2009.

547

548

Relative wind direction (°)	wind speed bias at $z - \Delta z$ (%)	Δz (m)
-20	2.98	1.44
-10	0.41	1.35
0	-0.39	1.32
10	-0.86	1.41
20	0.7	1.54
30	2.92	1.76
50	5.11	2.27
70	4.86	2.73
90	8.35	2.96
110	6.97	3.15

549

550 Table B1. Variation of wind speed bias and vertical flow displacement with relative wind
551 direction, determined at the location of the AutoFlux anemometer (height above sea level, z,
552 16.5 m). The wind speed bias and Δz are relative to a free stream location 2 seconds upstream
553 of the anemometer site (after Yelland et al., 2002). A negative relative wind direction
554 indicates a flow over the port side. Further details are given in Moat and Yelland (2015).
555
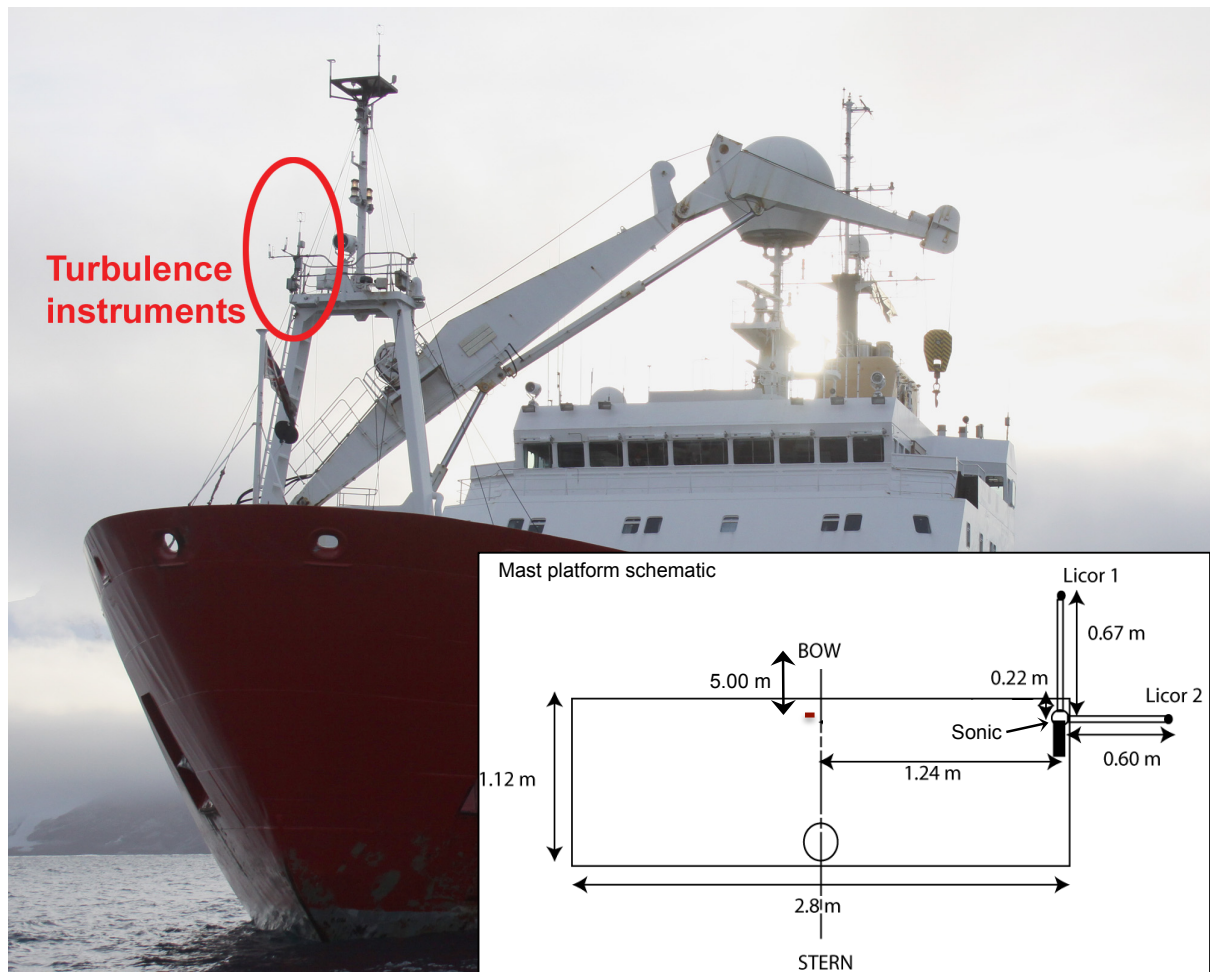
Figure 1. Locations of the flux instrumentation on the *RRS James Clark Ross*. The sonic anemometer is 2.0 m above the starboard forward corner of the platform. Note that the forecastle crane is generally stowed close to the deck while the ship is underway or on station.
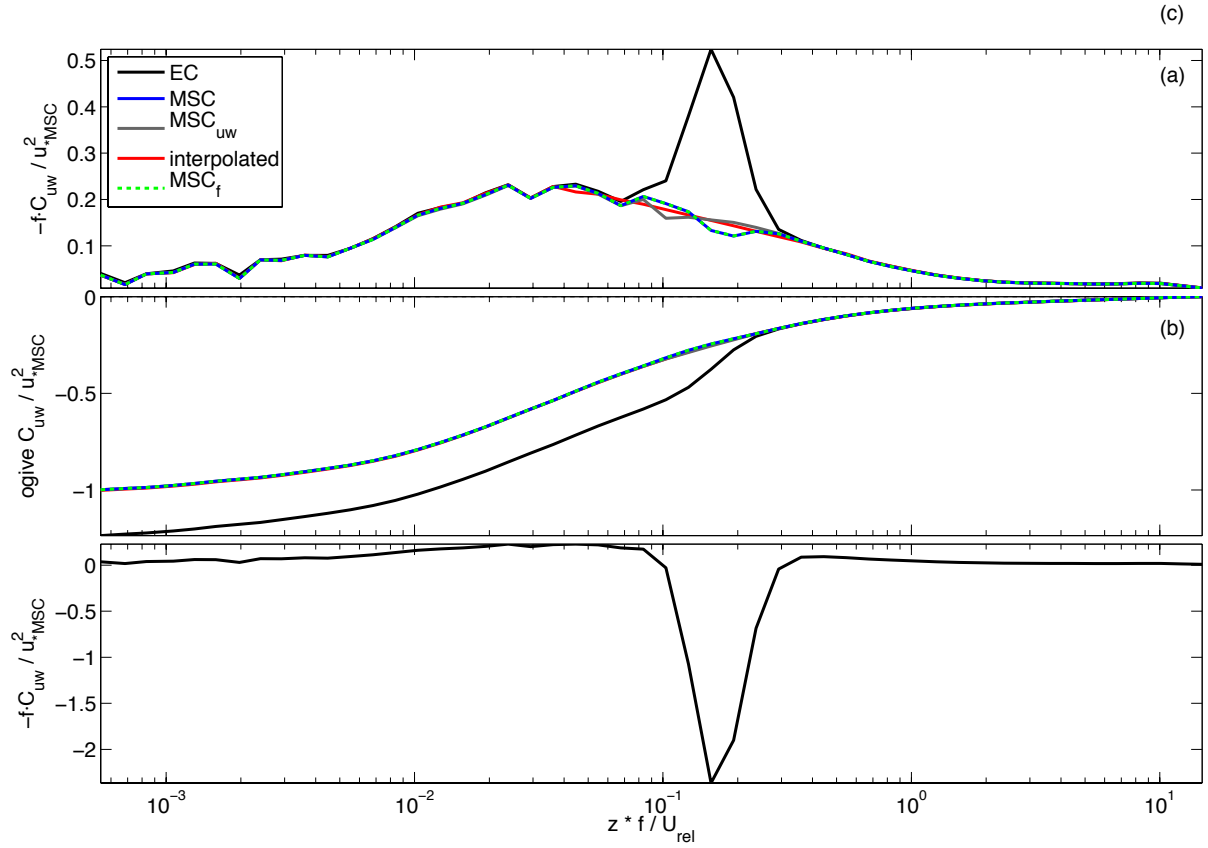
Figure 2. Frequency-weighted inverted and normalised momentum flux cospectra (a) and normalised ogives (b), shown relative to frequency non-dimensionalised using measurement height z and mean relative wind speed U_{rel}. Also shown are frequency-weighted, inverted and normalised cospectra calculated prior to motion correcting the turbulent velocity components, which results in a large upwards flux signal at the motion scale (c). Results shown are an average of 131 30-minute duration measurements at mean wind speeds 10 m s^{-1} < U_{10n} < 14 m s^{-1}. EC indicates the cospectra after removing platform motion following Edson et al. (1998) and shows the residual signal at scales typical of the wave field. The interpolation across the wave scales has been applied between frequencies of 0.04 and 0.4 Hz. The motion-scale correction (MSC) can either be applied as per Eq. (2) (MSC), with Eq. (2) applied to both the along and vertical wind components (MSC$_{uw}$), or as described by Edson et al., (2011) (MSC$_f$). Normalisation of the five different sets of results is by u$_*$ with MSC applied as per Eq. (2). Note that the MSC$_f$ line overlies the MSC line at all frequencies, and the interpolated, MSC$_{uw}$ and EC lines for frequencies away from the motion-scale.
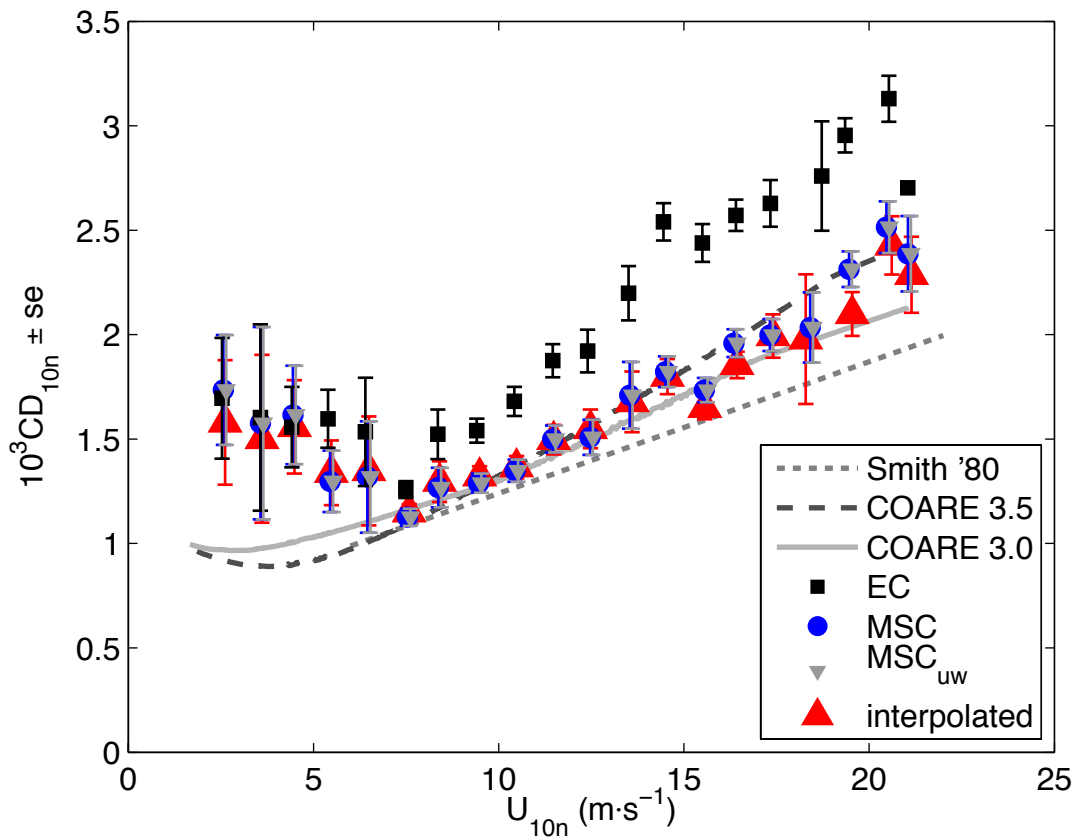
Figure 3. Drag coefficients bin-averaged by wind speed, relative to U_{10n} (n = 499).
Measurements are shown either without correction for wave-scale bias (EC), or with
correction applied to the vertical velocity only (MSC), both vertical and horizontal velocity
components (MSC$_{uw}$), or via a simple interpolation across the wave-scale portion of the
cospectra (interpolated). The bulk COARE 3.0 and 3.5 results are calculated without
dependence on wave field or radiation.
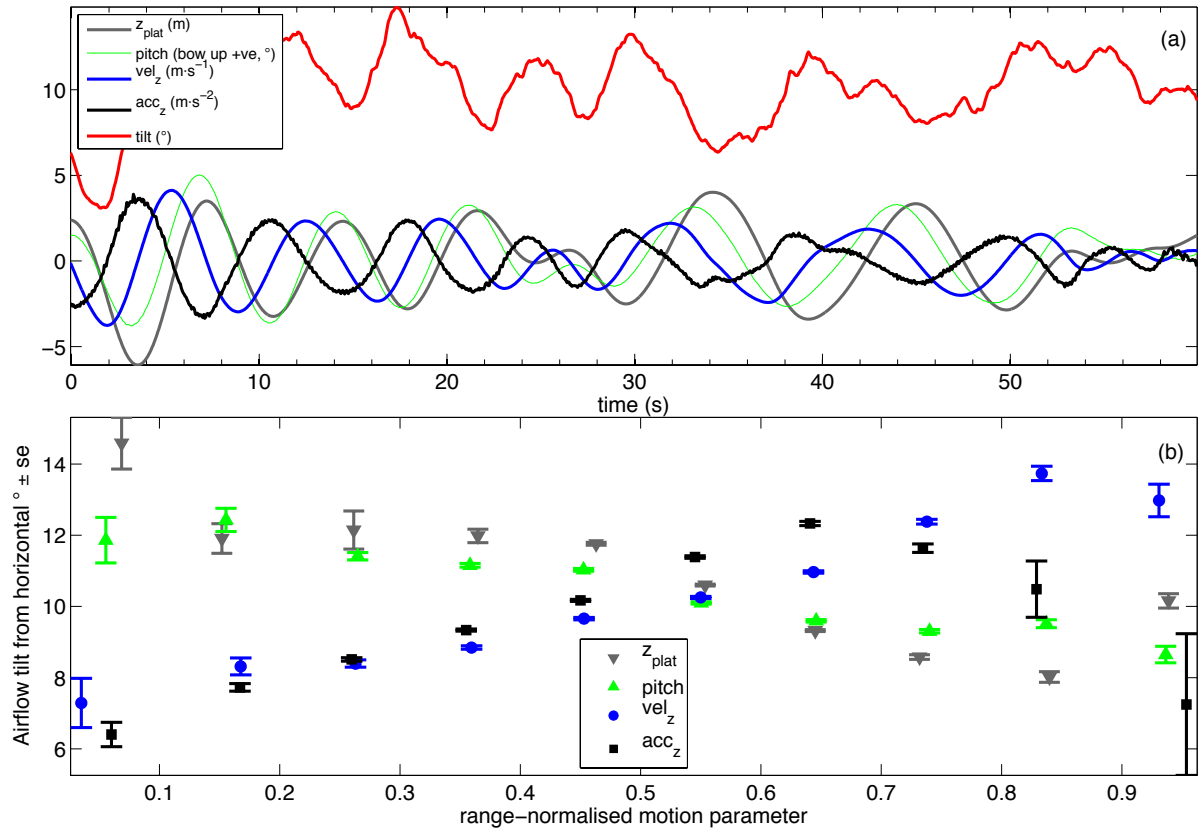
587 Figure 4. (a): Time series (60 s) of vertical platform displacement, velocity and acceleration,

588 platform pitch, and tilt from horizontal of the streamwise airflow measured by the AutoFlux

589 anemometer. The tilt has been smoothed with a 40-sample moving average. The

590 measurements are sampled from a period (23 April 2013, 21:00-21:30 UTC) with near bow-

591 on winds and mean U_{10n} of 15.2 m s^{-1}. (b): Variation of the tilt of streamwise airflow from

592 horizontal, relative to the vertical platform displacement, velocity, acceleration and platform

593 pitch each normalised by their measured range. Tilt averages were made over the 30-minute

594 period that the measurements in (a) were sampled from.

595
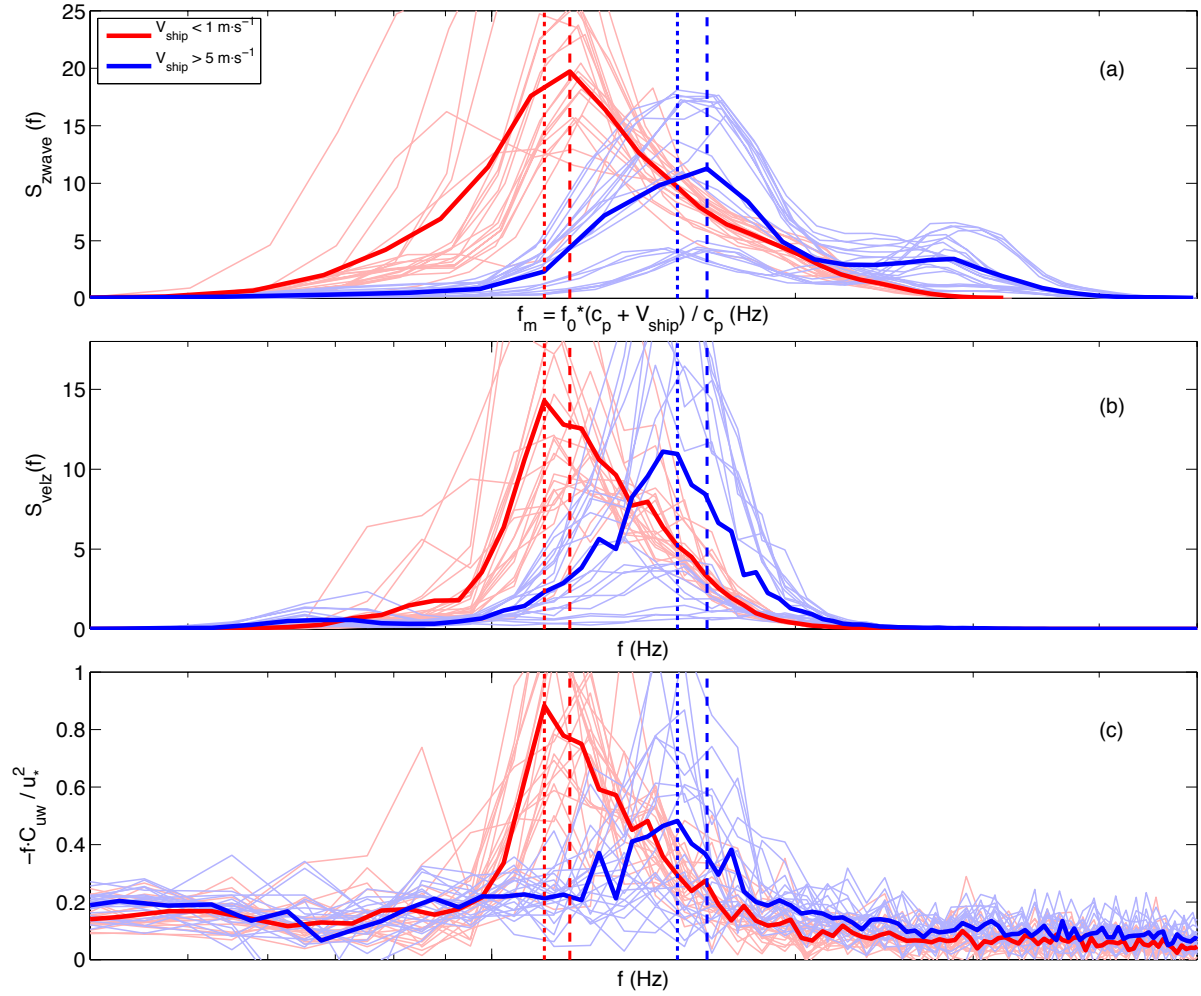
Figure 5. Comparison of averaged spectra. In all panels two sets of averaged data are compared, periods when the ship was stationary ($V_{ship} < 1$ m s^{-1}, 21 periods) and periods when the ship was steaming ($V_{ship} > 5$ m s^{-1}, 20 periods); the individual spectra are shown as pale lines for reference. For all measurements, U_{10n} was between 10 and 12 m s^{-1}. (a) Spectral density of non-directional wave heights from WAVEX with frequency shifted to the reference frame of the moving ship; (b) spectral density of platform vertical velocity as measured on the foremast; (c) frequency-weighted inverted cospectral density for the momentum flux (positive upwards) – turbulent velocity components are motion corrected, but the MSC correction is not applied. The dashed vertical lines indicate the peak frequency of the wave spectrum; dotted vertical lines indicate the peak frequency of the momentum flux cospectra in (c). Note that the axis limits are set very close to the scale of the ship motion to allow details to be seen clearly.
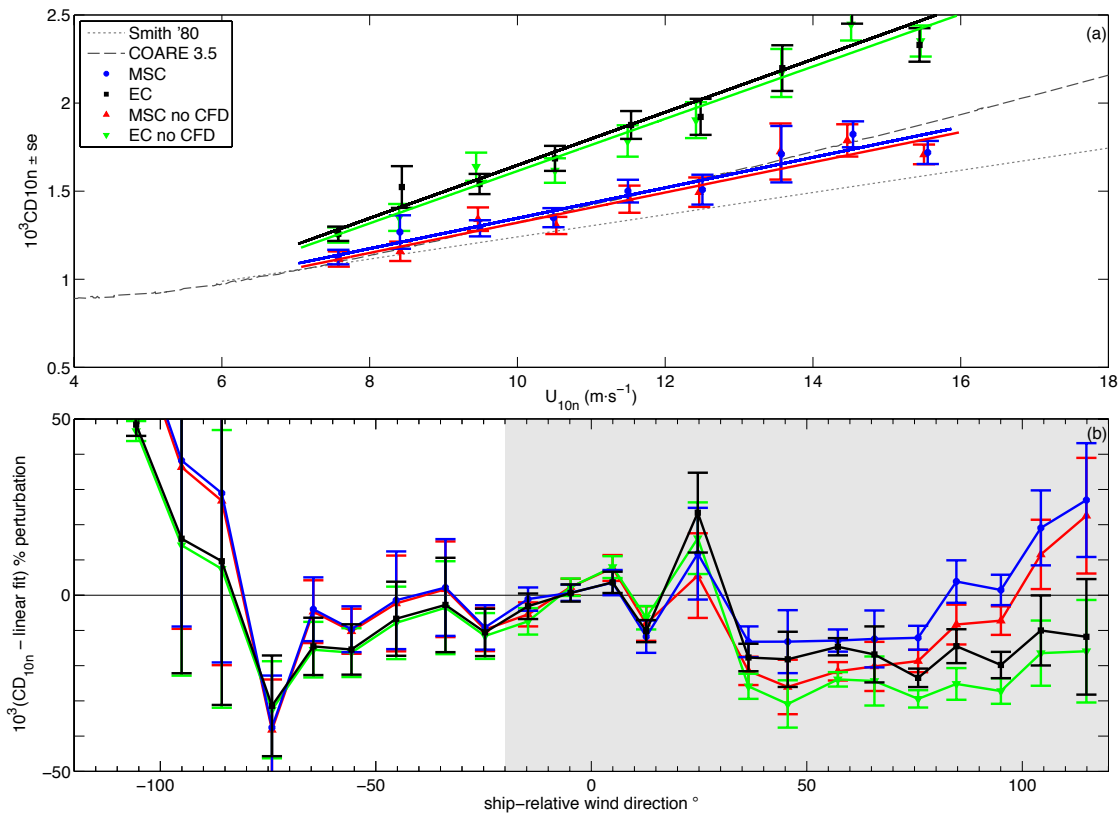
Figure 6. (a): Measurements either without correction for wave-scale bias (EC), or with correction applied to the vertical velocity only (MSC) for wind speeds 7 m s^{-1} < U_{10n} < 16 m s^{-1} (n = 335), and relative wind directions between -20° and +50° (where a wind on the bow is at 0°). Lines are linear fits to the measurements. (b): variation of the difference between measured drag coefficients and the linear fits against relative wind direction for the same wind speed criteria (n = 663). Both panels also show measurements (with and without MSC) which have not had CFD-derived corrections to mean wind speed and height applied. Note that CFD corrections were only applied for the shaded range.

619
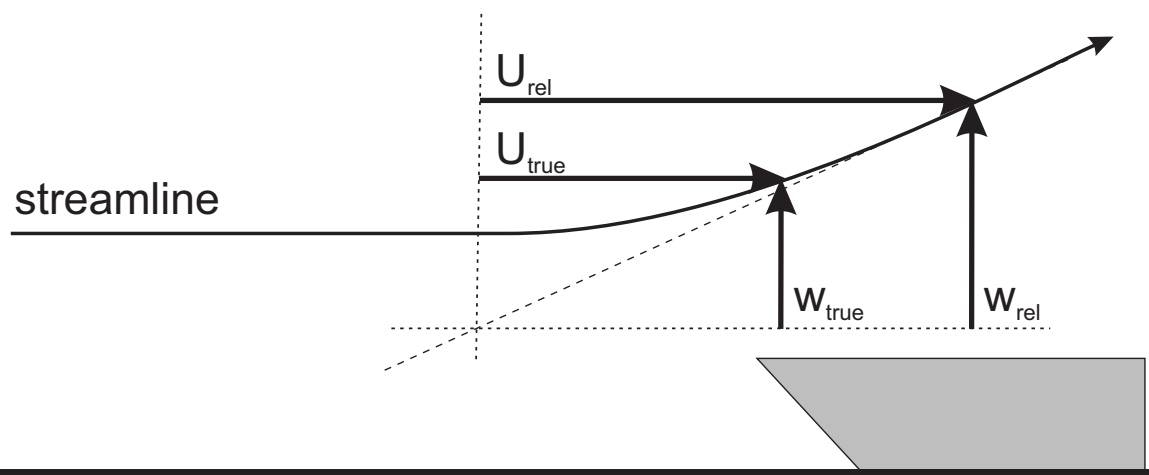
Figure A1. Schematic of the impact of ship horizontal velocity on non-horizontal airflow. The measured horizontal (U_{rel}) and vertical (w_{rel}) wind components must both be corrected for ship velocity to obtain the true wind components. Not correcting the measured vertical wind will result in an incorrect determination of the tilt angle of the flow from horizontal.
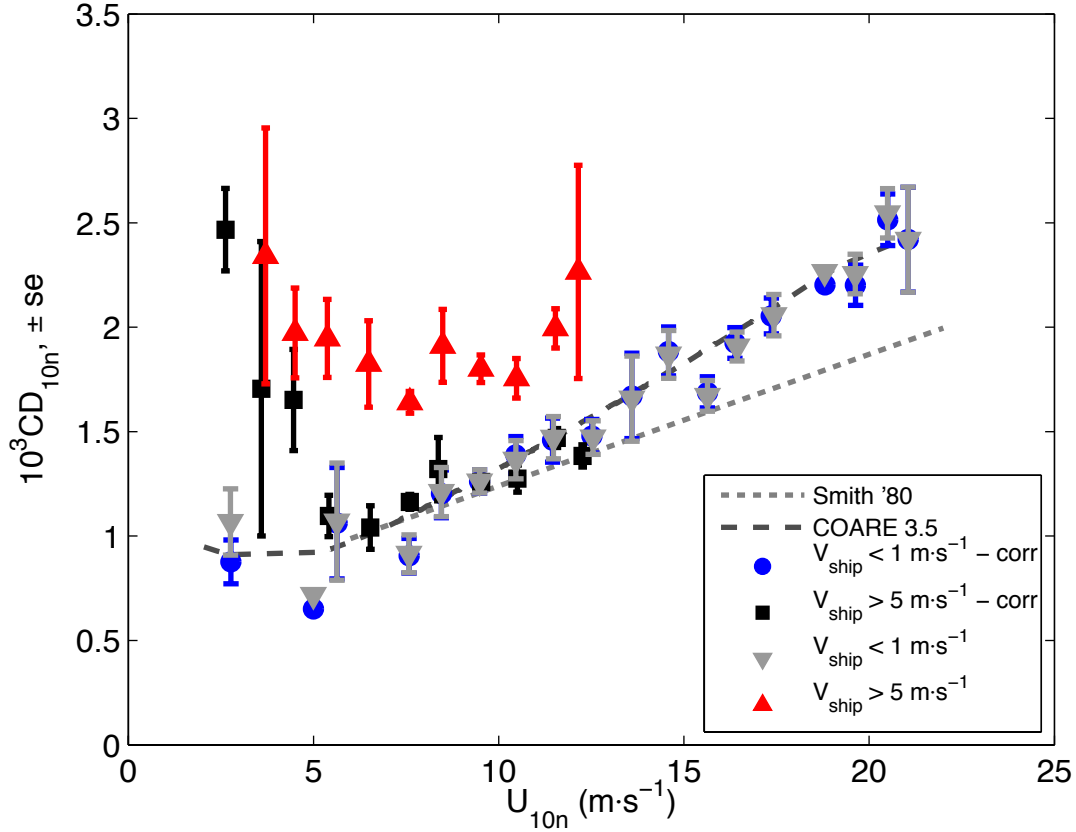
626
627 Figure A2. Wind speed-averaged drag coefficients, relative to U_{10n}. Two sets of

628 measurements are compared: where the ship was deemed stationary ($V_{ship} < 1$ m s^{-1}, n = 233);

629 and where the ship was underway ($V_{ship} > 5$ m s^{-1}, n = 182). The measurements are shown

630 with ('corr') and without the vertical wind speed corrected as per Eq. (1).

631